

## General Disclaimer

### One or more of the Following Statements may affect this Document

- This document has been reproduced from the best copy furnished by the organizational source. It is being released in the interest of making available as much information as possible.
- This document may contain data, which exceeds the sheet parameters. It was furnished in this condition by the organizational source and is the best copy available.
- This document may contain tone-on-tone or color graphs, charts and/or pictures, which have been reproduced in black and white.
- This document is paginated as submitted by the original source.
- Portions of this document are not fully legible due to the historical nature of some of the material. However, it is the best reproduction available from the original submission.

# NASA TECHNICAL MEMORANDUM

NASA TM -78129

## PRELIMINARY ASSESSMENT OF THE VACUUM ENVIRONMENT IN THE WAKE OF LARGE SPACE VEHICLES

By W. A. Oran and R. J. Naumann  
Space Sciences Laboratory

(NASA-TM-78129) PRELIMINARY ASSESSMENT OF  
THE VACUUM ENVIRONMENT IN THE WAKE OF LARGE  
SPACE VEHICLES (NASA) 34 p HC A03/MF A01  
CSCL 22A

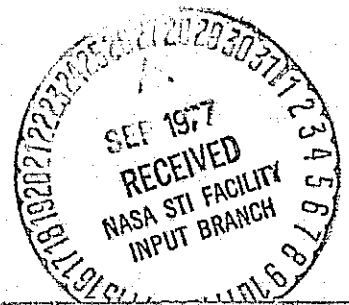
N77-31222

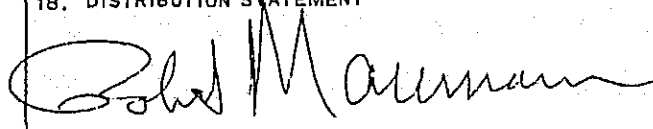
Unclas  
46260  
G3/15

July 1977

NASA

*George C. Marshall Space Flight Center  
Marshall Space Flight Center, Alabama*



1. REPORT NO. NASA TM-78129	2. GOVERNMENT ACCESSION NO.	3. RECIPIENT'S CATALOG NO.	
4. TITLE AND SUBTITLE Preliminary Assessment of the Vacuum Environment in the Wake of Large Space Vehicles		5. REPORT DATE July 1977	6. PERFORMING ORGANIZATION CODE
		8. PERFORMING ORGANIZATION REPORT #	
7. AUTHOR(S) W. A. Oran and R. J. Naumann		10. WORK UNIT NO.	
9. PERFORMING ORGANIZATION NAME AND ADDRESS George C. Marshall Space Flight Center Marshall Space Flight Center, Alabama 35812		11. CONTRACT OR GRANT NO.	
		13. TYPE OF REPORT & PERIOD COVERED Technical Memorandum	
12. SPONSORING AGENCY NAME AND ADDRESS National Aeronautics and Space Administration Washington, D. C. 20546		14. SPONSORING AGENCY CODE	
		15. SUPPLEMENTARY NOTES  Prepared by Space Sciences Laboratory, Science and Engineering	
16. ABSTRACT  The vacuum environment in the wake region of presently planned large space vehicles is calculated using simplified models of the particle fluxes from the various sources. The fluxes which are calculated come directly from the ambient, are due to ambient particles backscattered from spacecraft emissions, and are due to self-scattering of spacecraft emissions. Using nominal values for the surface emissions, the flux density environment behind a large unmanned craft at 550 km altitude is calculated at $\sim 10^7/\text{cm}^2 \text{ s}$ . For an experiment involving rapid physical deposition of vaporized material, this may result in contamination levels of $< 1$ part in $10^9$ occurring in the bulk material. Calculations indicate that the flux density on a wake vacuum experiment conducted in the vicinity of the Shuttle will be substantially greater than that behind unmanned craft. However, it is possible that, under appropriate circumstances, meaningful wake vacuum experiments still could be conducted using the Shuttle facilities.			
17. KEY WORDS		18. DISTRIBUTION STATEMENT    Unclassified — Unlimited	
19. SECURITY CLASSIF. (of this report)  Unclassified	20. SECURITY CLASSIF. (of this page)  Unclassified	21. NO. OF PAGES  34	22. PRICE  NTIS

# TABLE OF CONTENTS

	Page
I. INTRODUCTION . . . . .	1
II. AMBIENT PARTICLES WHICH DIRECTLY STRIKE A SURFACE ORIENTED TOWARDS THE WAKE . . . . .	3
III. INDUCED BACKSCATTERING OF AMBIENT PARTICLES BY SPACECRAFT EMISSIONS . . . . .	9
IV. SELF-SCATTERING OF SPACECRAFT EMISSIONS . . . . .	16
V. FLUXES IN THE WAKE REGION DUE TO OTHER PHENOMENA . . . . .	23
VI. DISCUSSION . . . . .	25
VII. CONCLUSIONS . . . . .	28
REFERENCES . . . . .	24

## LIST OF ILLUSTRATIONS

Figure	Title	Page
1.	Diagram of a spherical model of a satellite traversing the ionosphere and having an experiment mounted on the wake axis . . . . .	2
2.	Simplification of the model of Figure 1 where the experiment is replaced by a flat disc of radius $R_0$ . . . . .	3
3.	Diagram of appropriate velocity vectors and angles in a transformation from the c.m. to the spacecraft reference frames . . . . .	13
4.	Geometry relating to the self-scattering of spacecraft emissions . . . . .	16

## LIST OF TABLES

Table	Title	Page
1.	Flux of Ambient Particles per Unit Solid Angle as a Function of Angle to the Wake Axis $\theta$ . . . . .	7
2.	Flux of Ambient Particles per Unit Solid Angle as a Function of Angle to the Axis ( $\theta$ ) for a Flat Plate Oriented Toward the Wake . . . . .	8
3.	Flux of Backscattered Ambient per Unit Solid Angle as a Function of Angle ( $\theta$ ) to the Axis for a Flat Plate Oriented Toward the Wake . . . . .	15

## PRELIMINARY ASSESSMENT OF THE VACUUM ENVIRONMENT IN THE WAKE OF LARGE SPACE VEHICLES

### I. INTRODUCTION

The era of spaceflight (beginning with the launch of the first satellite in the late 1950's) has yielded a rich harvest in terms of the resultant advances in both science and technology. The long distance telephone communication system utilizing satellite relay and the use of satellite weather photographs by television meteorologists are but two of the better known examples. Perhaps one of the most beneficial and promising aspects of spaceflight is the ability to examine phenomena under conditions which cannot be duplicated in a cost-effective manner utilizing Earth-based facilities. For example, the field of X-ray astronomy, which needs to be conducted "above" the Earth's atmosphere, is a product of the space age. The discovery of celestial X-ray events has resulted in a virtual explosion of theories/ideas of cosmological importance and may ultimately result in a major revision of our present understanding of the laws of the universe.

In a similar vein, the capability to conduct long-duration experiments under zero-gravity conditions has resulted in a better understanding of a multitude of formation and separation processes. In fact, the results of the precursor investigations (conducted in the era of Apollo/Skylab) are so promising that follow-on experiments are being planned for the forthcoming era of the Shuttle/Spacelab to see if various materials and biological processes can be commercially undertaken in space [1].

Another unique in situ capability, which has only recently been reported, is the generation of the ultrahigh vacuum in the wake region of a space vehicle [2]. Some calculations examining the environment in the area within an actively controlled, ultraclean hemisphere indicate that particle densities  $\lesssim 10^3/\text{cm}^3$  may be obtainable in this zone [3].

This report will examine the contaminating fluxes from the ambient atmospheric molecules observed in the wake region of presently planned spacecraft [e. g. , Shuttle, Spacelab, Long Duration Exposure Facility (LDEF)] in order to help determine the vacuum levels that may be utilized by an experiment mounted on the "lee" portion of the vehicle. It will also discuss in a general manner some precursor experiments which could be conducted "relatively inexpensively" on these craft and which could help establish the usefulness/appliability of using the ultravacuum in the wake of a spacecraft.

To help evaluate experimental conditions, simplified models will be developed which will depict the contribution of various sources to the flux density in the wake. These contributions will be evaluated using typical spacecraft parameters. To help calculate the flux densities, a model spacecraft which approximates large unmanned spacecraft such as LDEF will be used. It is an approximately spherical body, with radius  $R_0 = 2$  m, traversing the upper atmosphere at velocity  $V_0 \sim 7.8$  km/s at a nominal altitude of  $\sim 550$  km (Fig. 1).

An experiment utilizing the wake vacuum is mounted on the rear portion of the satellite. At 550 km the nominal parameters of the neutral ambient atmosphere used in the calculations are: temperature,  $T \sim 1000$  K; density of oxygen,  $O \sim 8 \times 10^6/\text{cm}^3$ ; density of helium,  $He \sim 2 \times 10^6/\text{cm}^3$ ; and density of hydrogen,  $H \sim 5 \times 10^4/\text{cm}^3$  [4]. In addition, to assess in a semiquantitative fashion the fluxes which can strike an experiment mounted in the wake, the experimental area will be approximated by a flat plate.

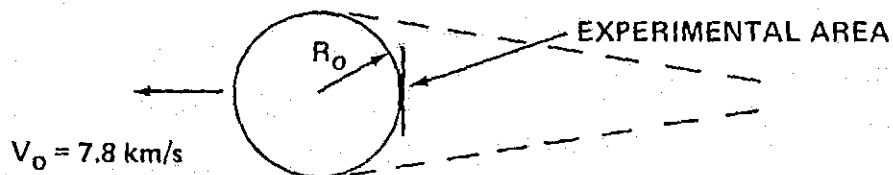


Figure 1. Diagram of a spherical model of a satellite traversing the ionosphere and having an experiment mounted on the wake axis.

## II. AMBIENT PARTICLES WHICH DIRECTLY STRIKE A SURFACE ORIENTED TOWARDS THE WAKE

The velocity shifted Maxwellian distribution  $f(v)$  can be used to evaluate that portion of the ambient flux which has a velocity sufficient to overtake a spacecraft where

$$f(v) = N \left( \frac{m}{2\pi KT} \right)^{3/2} \exp \left[ -\frac{m}{2KT} (V_\phi^2 + (V_r - V_o \cos \theta)^2 + (V_\theta + V_o \sin \theta)^2) \right] dV_r dV_\theta dV_\phi \quad (1)$$

and  $N$  = particle density.

The terms  $r$ ,  $\theta$ ,  $\phi$  are polar angles as shown in Figure 2, and the remaining symbols have a standard meaning. Based on intuition, one would anticipate the flux of particles per unit solid angle ( $\sin \theta d\theta d\phi$ ) to increase as the angle increases from the wake to the ram direction. To help assess the ability of conical/hemispherical shapes in reducing this contribution to the flux density in the wake, we will first calculate

$$\text{flux density } (\theta) = F(\theta)$$

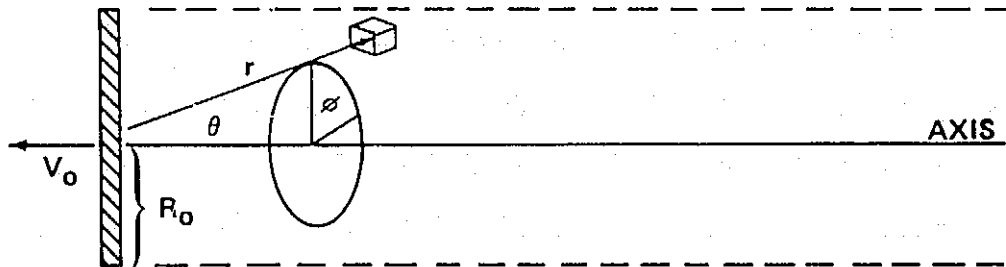


Figure 2. Simplification of the model of Figure 1 where the experiment is replaced by a flat disc of radius  $R_o$ .



(The angular relations are given in Figure 2.) The flux of ambient particles coming in for a given  $\theta$  at solid angle ( $\sin \theta d\theta d\phi$ ) is then

$$F(\theta) = \int_0^{\infty} dV_r \int_{\text{allowable}} dV_{\theta} \int_{\text{allowable}} dV_{\phi} V_r f(v)$$

Only those particles whose  $V_{\theta}$  and  $V_{\phi}$  components of velocities are in the range

$$-V_r \tan\left(\frac{\sin \theta d\phi}{2}\right) \leq V_{\phi} \leq V_r \tan\left(\frac{\sin \theta d\phi}{2}\right)$$

and

$$V_r \tan\left(\frac{d\theta}{2}\right) \leq V_{\theta} \leq V_r \tan\left(\frac{d\theta}{2}\right)$$

can reach the surface from the specified solid angle ( $\sin \theta d\theta d\phi$ ) at angle  $\theta$ , or

$$F(\theta) = \left\{ N \left( \frac{m}{2\pi KT} \right)^{3/2} \int_0^{\infty} V_r \exp \left[ -\frac{m}{2KT} (V_r - V_0 \cos \theta)^2 \right] dV_r \right\} \times$$

$$\left\{ \int_{-V_r \tan\left(\frac{\sin \theta d\phi}{2}\right)}^{V_r \tan\left(\frac{\sin \theta d\phi}{2}\right)} dV_{\phi} \int_{-V_r \tan\left(\frac{d\theta}{2}\right)}^{V_r \tan\left(\frac{d\theta}{2}\right)} dV_{\theta} \exp \left( -\frac{m}{2KT} [V_{\phi}^2 + (V_{\theta} + V_0 \sin \theta)^2] \right) \right\}$$

Assuming that  $d\theta$ ,  $d\phi \ll 1$ , we can utilize the approximations

$$V_r \tan \left( \frac{\sin \theta d\phi}{2} \right) \sim V_r \frac{\sin \theta d\phi}{2} \ll \left( \frac{2kT}{m} \right)^{1/2},$$

$$V_r \tan \left( \frac{d\theta}{2} \right) \sim V_r \frac{d\theta}{2} \ll \left( \frac{2kT}{m} \right)^{1/2},$$

and

$$V_r V_o \sin \theta d\theta \ll \left( \frac{2kT}{m} \right).$$

Then

$$F(\theta) \sim N \left( \frac{m}{2\pi kT} \right)^{3/2} \sin \theta d\theta d\phi \exp \left( - \frac{mV_o^2 \sin^2 \theta}{2kT} \right)$$

$$\int_0^{\infty} V_r^3 \exp \left[ - \frac{m}{2kT} (V_r - V_o \cos \theta)^2 \right] dV_r$$

$$F_o(\theta) = \frac{F(\theta)}{\sin \theta d\theta d\phi} \sim N \left( \frac{m}{2\pi kT} \right)^{3/2} \exp \left( - \frac{mV_o^2 \sin^2 \theta}{2kT} \right)$$

$$\int_0^{\infty} V_r^3 \exp \left[ - \frac{m}{2kT} (V_r - V_o \cos \theta)^2 \right] dV_r \quad (2)$$

Equation (2) can be explicitly solved and an analytic solution for  $F_o$  found. However, it was more convenient to solve equation (2) using a computer. The results of these calculations are shown in Table 1 for three different atmospheric constituents (hydrogen, helium, and oxygen) under standard atmospheric conditions at 550 km.

The results in Table 1 show that the flux  $F_o(\theta)$  does indeed increase by orders of magnitude as  $\theta$  varies in the range 0 to 90 degrees. Therefore, some kind of conical or quasi-spherical shape around the experimental area could be used to reduce the direct flux of the ambient atmosphere. However, it is also useful to find the flux impinging on a flat plate (Fig. 2) to help assess (in a semiquantitative fashion) the influence this direct ambient flux has on the flux density seen by a "flat" experiment. This is done utilizing the expression  $F_o'(\theta) = F_o(\theta) \cos \theta$ , and the results are presented in Table 2. Similarly, it is of interest to calculate the total flux impinging on a flat plate (Fig. 2). Utilizing the expression

$$F_o = \int_0^{2\pi} d\phi \int_0^{\pi} \sin\theta d\theta F_o(\theta)$$

and then numerically integrating the results of Table 2, we obtain:

$$F_o(H) \sim 1.1 \times 10^7 / \text{cm}^2 \text{ s}$$

$$F_o(\text{He}) \sim 10^3 / \text{cm}^2 \text{ s}$$

$$F_o(O) < 1 / \text{cm}^2 \text{ s}$$

As a check upon the accuracy of some of the approximations mentioned previously, we note that the results of this numerical integration are in good agreement with the results from the analytic expression

$$F_o = N \left( \frac{KT}{2\pi m} \right)^{1/2} \left\{ e^{-\frac{mV_o^2}{2KT}} - \left( \frac{\pi m}{KT} \right)^{1/2} V_o \left( 1 - \operatorname{erf} \left[ \frac{V_o}{(2KT/m)^{1/2}} \right] \right) \right\}$$

which describes the flux to a flat plate oriented toward the wake axis [3].

TABLE 1. FLUX OF AMBIENT PARTICLES PER UNIT SOLID ANGLE AS A FUNCTION OF ANGLE TO THE WAKE AXIS  $\theta^a$

Angle (degree)	Flux		
	H ( $\text{cm}^2 \text{ s}$ )	He ( $\text{cm}^2 \text{ s}$ )	O ( $\text{cm}^2 \text{ s}$ )
0	$10^6$	30	$4 \times 10^{-19}$
10	$10^6$	30	$4 \times 10^{-19}$
20	$10^6$	40	$5 \times 10^{-19}$
30	$1.5 \times 10^6$	60	$6 \times 10^{-19}$
40	$2 \times 10^6$	80	$10^{-18}$
50	$3 \times 10^6$	$1.5 \times 10^2$	$2 \times 10^{-18}$
60	$5 \times 10^6$	$3 \times 10^2$	$5 \times 10^{-18}$
70	$9 \times 10^6$	$7.5 \times 10^2$	$2 \times 10^{-17}$
80	$2 \times 10^7$	$2.5 \times 10^3$	$10^{-16}$
90	$4 \times 10^7$	$1.3 \times 10^4$	$2 \times 10^{-15}$
100	$10^8$	$10^5$	$2 \times 10^{-13}$
110	$3 \times 10^8$	$10^6$	$1.5 \times 10^{-10}$
120	$9 \times 10^8$	$2 \times 10^7$	$10^{-6}$
130	$2.5 \times 10^9$	$4 \times 10^8$	$3 \times 10^{-2}$
140	$7 \times 10^9$	$7 \times 10^9$	$10^3$
150	$2 \times 10^{10}$	$10^{11}$	$3 \times 10^7$
160	$3.5 \times 10^{10}$	$10^{12}$	$10^{11}$
170	$5.5 \times 10^{10}$	$4 \times 10^{12}$	$2 \times 10^{13}$
180	$6 \times 10^{10}$	$7 \times 10^{12}$	$10^{14}$

- a. The model used assumes an ambient temperature  $\sim 1000 \text{ K}$  and following ambient densities: O  $\sim 8 \times 10^6/\text{cm}^3$ , He  $\sim 2 \times 10^6/\text{cm}^3$ , and H  $\sim 5 \times 10^4/\text{cm}^3$ .

TABLE 2. FLUX OF AMBIENT PARTICLES PER UNIT SOLID ANGLE AS A FUNCTION OF ANGLE TO THE AXIS ( $\theta$ ) FOR A FLAT PLATE ORIENTED TOWARD THE WAKE<sup>a</sup>

Angle (degree)	Flux		
	H (cm <sup>2</sup> s)	He (cm <sup>2</sup> s)	O (cm <sup>2</sup> s)
0	10 <sup>6</sup>	30	4 × 10 <sup>-19</sup>
10	10 <sup>6</sup>	30	4 × 10 <sup>-19</sup>
20	10 <sup>6</sup>	40	4.7 × 10 <sup>-19</sup>
30	1.3 × 10 <sup>6</sup>	50	5 × 10 <sup>-19</sup>
40	1.5 × 10 <sup>6</sup>	60	8 × 10 <sup>-19</sup>
50	2 × 10 <sup>6</sup>	10 <sup>2</sup>	1.2 × 10 <sup>-18</sup>
60	2.5 × 10 <sup>6</sup>	1.5 × 10 <sup>2</sup>	2.5 × 10 <sup>-18</sup>
70	3 × 10 <sup>6</sup>	2.5 × 10 <sup>2</sup>	7 × 10 <sup>-18</sup>
80	3.5 × 10 <sup>6</sup>	4 × 10 <sup>2</sup>	10 <sup>-17</sup>
90	—	—	—

a. The model used assumes an ambient temperature ~ 1000 K and the following ambient densities: O ~ 8 × 10<sup>6</sup>/cm<sup>3</sup>, He ~ 2 × 10<sup>6</sup>/cm<sup>3</sup>, and H ~ 5 × 10<sup>4</sup>/cm<sup>3</sup>. The calculation includes the cos  $\theta$  factor of flux to a flat surface.

### III. INDUCED BACKSCATTERING OF AMBIENT PARTICLES BY SPACECRAFT EMISSIONS

To calculate this contribution to the flux density in the wake, we will utilize the same geometrical orientation as used in Section II (see Fig. 2). Let the flux density of molecules emitted by the spacecraft equal  $N_o / 4\pi r^2 V_T$ , be  $N_o(r)$ , and be independent of  $\theta$ . The collision rate in volume element  $dv$  between the ambient and emitted particles is equal to<sup>1</sup>

$$N N_o(r) / \vec{V}_T - \vec{V}_o / \sigma_{Ao} dv$$

where

$N$  = ambient density

$V_o$  = velocity of ambient particles in spacecraft reference frame  
 $\sim 7.8 \text{ km/s}$

$V_T$  = velocity of emitted particles

$\sigma_{Ao}$  = collision cross section

$$dv = r^2 \sin \theta d\theta d\phi$$

$$V_o \gg V_T$$

$N_o$  = spacecraft emission rate (molecules/s).

The number of ambient particles that scatter back to the surface is  $F_{IB}$ , where

$$F_{IB}(r, \theta, \phi) = N N_o(r) V_o \left( \frac{d\sigma}{d\Omega} \right)_{\pi-\theta}^{s/c} r^2 \sin \theta d\theta d\phi \frac{A \cos \theta}{r^2}$$

1. For this model a cold beam flow is assumed, where all the ambient molecules have initial velocities parallel to the wake axis.

$$A = \pi R_o^2 ,$$

and

$$\left( \frac{d\sigma}{d\Omega} \right)_{\pi-\theta}^{s/c}$$

is the differential cross section ( $\sigma_{Ao}$  times the probability the ambient particle will be scattered into unit solid angle in direction  $\pi - \theta$ ). The foregoing equation can be integrated over  $r$  to yield

$$F_{IB}(\theta, \phi) = \frac{N_o N_o V_o}{4\pi V_T} \left( \frac{d\sigma}{d\Omega} \right)_{\pi-\theta}^{s/c} A \sin \theta \cos \theta d\theta d\phi \int_{r_1(\theta)}^{\infty} \frac{dr}{r^2}$$

where  $r_1(\theta)$  is the distance behind the body at which the ambient density again becomes significant; i. e. ,

$$r_1(\theta) \sim r_o / \sin \theta$$

or

$$F_{IB}(\theta, \phi) \sim \frac{N_o N_o V_o A}{4\pi V_T R_o} \left( \frac{d\sigma}{d\Omega} \right)_{\pi-\theta}^{s/c} \sin^2 \theta \cos \theta d\theta d\phi .$$

The term

$$\left( \frac{d\sigma}{d\Omega} \right)_{\pi-\theta}^{s/c}$$

can best be evaluated by transformation to the center of mass (c.m.) system. Since  $V_o \gg V_T$ , we find

$$V_{c.m.} \sim \frac{V_o m_o}{m_o + m_a}$$

$$V_{o,c.m.} \sim V_o - V_{c.m.}$$

where  $m_a$  = mass of emitted particle,  $m_o$  = mass of ambient particle, and after collision

$$V_{o,c.m.}^2 \sim \frac{m_o (V_o - V_{c.m.})^2 + m_a (V_{c.m.})^2 - 2Q}{\left( m_o + \frac{m_o^2}{m_a} \right)}$$

where  $Q$  is the translational energy loss in the collision. Also in the c.m. system, assuming a hard sphere model for the collision,

$$\left( \frac{d\sigma}{d\Omega} \right)_{o^*}^{c.m.} = \frac{\sigma A_o}{4\pi}$$

The differential cross section in the c.m. is related to that in the spacecraft reference frame by

$$\left( \frac{d\sigma}{d\Omega} \right)_{\pi-0}^{s/c} = \left( \frac{d\sigma}{d\Omega} \right)_{o^*}^{c.m.} \frac{\sin \theta^* d\theta^*}{\sin \theta d\theta} = \frac{\sigma A_o}{4\pi} \frac{\sin \theta^* d\theta^*}{\sin \theta d\theta}$$



where we are assuming an isotropic scattering in the c.m. system. It can be similarly shown using Figure 3 that

$$d\theta^* = d\theta \left\{ 1 - \frac{\beta \cos \theta}{\sqrt{1 - \beta^2 \sin^2 \theta}} \right\}$$

and

$$\sin \theta^* = \sin \theta \left\{ \sqrt{1 - \beta^2 \sin^2 \theta} - \beta \cos \theta \right\} .$$

or

$$F_{\text{IB}}(\theta, \phi) = \frac{N N_0 V_0 \sigma_{A0}}{(4\pi)^2 V_{\text{T}0} R_0} \sin \theta d\theta d\phi G(\theta)$$

where

$$\beta = V_{\text{c.m.}} / V_{0, \text{c.m.}}^*$$

$$\beta = \left[ \frac{1 + \frac{m_0}{m_a}}{\left( \frac{V_0}{V_{\text{c.m.}}} - 1 \right)^2 + \frac{m_a}{m_0} - \frac{2Q}{m_0 V_{\text{c.m.}}^2}} \right]^{1/2}$$

and

$$G(\theta) = \sin \theta \cos \theta \left\{ 1 - \frac{\beta \cos \theta}{\sqrt{1 - \beta^2 \sin^2 \theta}} \right\} \left\{ \sqrt{1 - \beta^2 \sin^2 \theta} - \beta \cos \theta \right\} .$$

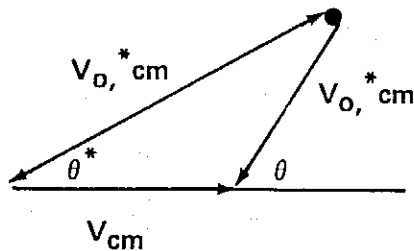


Figure 3. Diagram of appropriate velocity vectors and angles in a transformation from the c.m. to the spacecraft reference frames.

From the energetics of the collision it is obvious that scattered ambient particles cannot reach the wake surface unless  $V_{o,c.m.}^* > V_{c.m.}$  (i.e.,  $\beta < 1$ ).<sup>2</sup> For the case of elastic collisions,  $\beta$  is minimized (i.e.,  $Q = 0$ ) and becomes

$$\beta = \frac{m_o}{m_a}$$

Emissions from a spacecraft are usually  $H_2O$ ,  $N_2$ , and  $O_2$ , and we will assume a mean  $m_a \sim 24$  AMU. This yields

$$\beta_H = 0.042 \quad m_o = 1 \text{ AMU}$$

$$\beta_{He} = 0.167 \quad m_o = 4 \text{ AMU}$$

$$\beta_O = 0.75 \quad m_o = 16 \text{ AMU}$$

In a similar manner as Section II, we will calculate  $F_{IB}(\theta)$  per unit solid angle; i.e.,

$$\frac{F_{IB}(\theta)}{\sin \theta \, d\theta \, d\phi} \sim \frac{N_o N_c V_{Ao} \tau}{(4\pi)^2 V_T R_o} G(\theta)$$

2. For the outgassing molecules  $\beta$  is always greater than 1; consequently, for this model which assumes a cold particle flow, these molecules cannot be scattered upstream.

where N is calculated for atmosphere at 550 km,  $\sigma_{AO} \sim 3 \times 10^{-15} \text{ cm}^2$ , and  $N_O = n4\pi R_O^2$ ,  $R_O = 3 \text{ m}$ .  $n = \sim 10^{+12} \text{ molecules/cm}^2 \text{ s}$  which is estimated to be the emissions of unmanned spacecraft after days in orbit [5]. The results of these calculations are listed in Table 3.

It can be seen that unlike the flux densities calculated in Section II, the oxygen contribution is significant. The oxygen flux densities also vary approximately a factor of 10 over range of angles compared to the factor 2-3 for hydrogen and helium in Table 3.

The results in Table 3 can be integrated over the solid angle to yield the total flux impingement on the flat plate. The results are:

$$F_{IB} \text{ H} \sim 10^5 / \text{cm}^2 \text{ s}$$

$$F_{IB} \text{ He} \sim 3 \times 10^6 / \text{cm}^2 \text{ s}$$

$$F_{IB} \text{ O} \sim 3 \times 10^6 / \text{cm}^2 \text{ s}$$

It should be remembered that the estimates assume a worst case, i. e., completely elastic collisions ( $Q = 0$ ). If the energy loss for O colliding with  $\text{H}_2\text{O}$  is more than 11 percent (more than 43 percent for O colliding with  $\text{N}_2$ ),  $\beta \geq 1$  and no backscatter is possible. Since the energies available are more than sufficient to excite both rotational and vibrational states, some loss of translational energy is sure to occur. How much is difficult to estimate. In addition, this is a single collision model. For the parameter values discussed in this report, the mean free path of a spacecraft-emitted particle is  $\sim 20 \text{ km}$ , while less than 0.01 percent of the ambient molecules will collide with a spacecraft emission.

Since the backscattered flux is roughly  $\sim 1/r$ , we could expect that only those collisions which occur within 100 m of the body are significant. Given a mean free path of  $\sim 20 \text{ km}$ , it could be anticipated that multiple collisions would not be a factor in calculating the flux of backscattered particles. However, at the lower altitudes where the ambient density has greatly increased, the mean free path of the spacecraft emissions can be reduced to tens of meters, and the results of this model should be reevaluated to account for multiple collisions.

3. This value for  $\sigma_{AO}$  for oxygen interacting with the spacecraft emissions was determined for a water molecule. The cross section for water was calculated using the density of water  $\sim 1 \text{ gm/cm}^3$  and the number of molecules/gm.

TABLE 3. FLUX OF BACKSCATTERED AMBIENT PER UNIT SOLID ANGLE AS A FUNCTION OF ANGLE ( $\theta$ ) TO THE AXIS FOR A FLAT PLATE ORIENTED TOWARD THE WAKE<sup>a</sup>

Angle (degree)	Flux		
	O	He	H
10	$8 \times 10^4 / \text{cm}^2 \text{ s}$	$2.4 \times 10^5 / \text{cm}^2 \text{ s}$	$8 \times 10^3 / \text{cm}^2 \text{ s}$
20	$18 \times 10^4 / \text{cm}^2 \text{ s}$	$4.5 \times 10^5 / \text{cm}^2 \text{ s}$	$15 \times 10^3 / \text{cm}^2 \text{ s}$
30	$29 \times 10^4 / \text{cm}^2 \text{ s}$	$6.3 \times 10^5 / \text{cm}^2 \text{ s}$	$20 \times 10^3 / \text{cm}^2 \text{ s}$
40	$40 \times 10^4 / \text{cm}^2 \text{ s}$	$7.4 \times 10^5 / \text{cm}^2 \text{ s}$	$23 \times 10^3 / \text{cm}^2 \text{ s}$
50	$54 \times 10^4 / \text{cm}^2 \text{ s}$	$7.8 \times 10^5 / \text{cm}^2 \text{ s}$	$23 \times 10^3 / \text{cm}^2 \text{ s}$
60	$68 \times 10^4 / \text{cm}^2 \text{ s}$	$7.2 \times 10^5 / \text{cm}^2 \text{ s}$	$20 \times 10^3 / \text{cm}^2 \text{ s}$
70	$74 \times 10^4 / \text{cm}^2 \text{ s}$	$5.6 \times 10^5 / \text{cm}^2 \text{ s}$	$15 \times 10^3 / \text{cm}^2 \text{ s}$
80	$65 \times 10^4 / \text{cm}^2 \text{ s}$	$3.2 \times 10^5 / \text{cm}^2 \text{ s}$	$8 \times 10^3 / \text{cm}^2 \text{ s}$

a. The ambient data used are the same as those given in Table 1, and the calculations include the  $\cos \theta$  factor of flux to a flat surface.

## IV. SELF-SCATTERING OF SPACECRAFT EMISSIONS

In this section we are interested in calculating the return flux of the emissions to the spacecraft because of self-scattering of the emission cloud. We will assume a stationary sphere uniformly outgassing via a Lambertian pattern at rate  $\eta$  in a vacuum. The flux of molecules per unit solid angle leaving the surface seen at a point  $r'$  and angle  $\gamma$  from the normal of  $dA$  is

$$dF \sim \frac{\eta dA \cos \gamma}{\pi r'^2}$$

The density contribution from the circular element (Fig. 4) is

$$dN = \frac{dF}{\bar{v}} \sim \frac{a^2 \eta \cos \gamma 2\pi \sin \alpha d\alpha}{\pi \bar{v} r'^2}$$

where

$$\bar{v} = \left( \frac{8KT}{\pi m} \right)^{1/2}$$

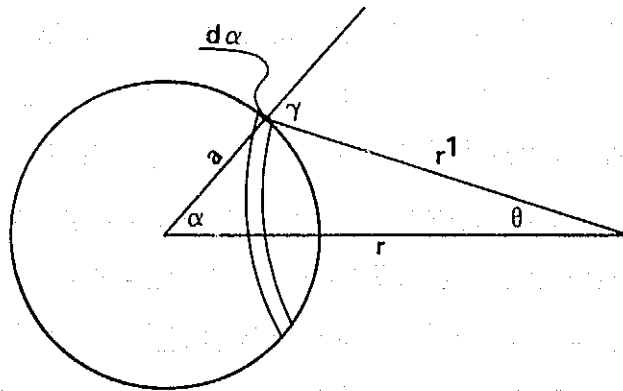


Figure 4. Geometry relating to self-scattering of spacecraft emissions.

The total density at  $r$  is then

$$N(r) = \frac{2\eta}{\bar{v}} \int_0^{\alpha} \frac{\cos \gamma \sin \alpha d\alpha}{(r'/a)^2}$$

where  $\alpha_0$  is determined from the solid angle of the sphere as seen at r. We know that

$$\frac{r'}{a} = \frac{\sin \alpha}{\sin \theta} = \frac{\sin(\gamma - \theta)}{\sin \theta} = \frac{\sin \gamma \cos \theta}{\sin \theta} - \cos \gamma$$

Let

$$\xi = \frac{r}{a} ;$$

then

$$\sin \gamma = \xi \sin \theta$$

or

$$\frac{r'}{a} = \xi \cos \theta - \cos \gamma$$

and

$$\cos \gamma = (1 - \xi^2 \sin^2 \theta)^{1/2}$$

and

$$d\alpha = d\gamma - d\theta = \left( 3 \frac{\cos \theta}{\cos \gamma} - 1 \right) d\theta = \left( \frac{r'}{a} \right) \frac{d\theta}{\cos \gamma}$$

Therefore, the integral becomes

$$N(r) = \frac{2\eta}{\bar{v}} \int_0^{\alpha_0} \frac{\cos \gamma \left( \frac{r'}{a} \right) \sin \theta \left( \frac{r'}{a} \right) d\theta}{\left( \frac{r'}{a} \right)^2 \cos \gamma} = \frac{2\eta}{\bar{v}} \int_0^{\alpha_0} \sin \theta d\theta$$

where

$$\theta_0 = \sin^{-1} \left( \frac{1}{\xi} \right)$$

or

$$N(r) = \frac{2\eta}{\bar{v}} (1 - \cos \theta_0) = \frac{2\eta}{\bar{v}} \left( 1 - \left( 1 - \frac{1}{\xi^2} \right)^{1/2} \right)$$

Note that as  $\xi \gg 1$ ,

$$N(r) \rightarrow \frac{2\eta}{\bar{v}} \left( \frac{1}{2\xi^2} \right) = \frac{\eta}{\bar{v}} \frac{a^2}{r^2}$$

which is the accepted equation to describe the density due to flux emission by a distant body.

To model the dynamics of the self-collision process, we will assume identical particles emitted at identical velocities  $\bar{v}$  and that for every collision occurring at  $r$ , the velocity  $\bar{v}(r)$  of the center of mass of the collision is average velocity of the emitted particles along the radial direction.

Utilizing Figure 1, we find

$$\begin{aligned} \bar{v}(r) &= \frac{\int_0^{\theta_0} \left( \frac{2\eta}{\bar{v}} \right) \bar{v} \cos \theta \sin \theta \, d\theta}{\int_0^{\theta_0} \left( \frac{2\eta}{\bar{v}} \right) \sin \theta \, d\theta} = \frac{\bar{v}}{2} \frac{\sin^2 \theta_0}{(1 - \cos \theta_0)} \\ &= \frac{\bar{v}}{2} (1 + \cos \theta_0) = \frac{\bar{v}}{2} \left( 1 + \left( 1 - \frac{1}{\xi^2} \right)^{1/2} \right) \end{aligned}$$

Note that as  $r \rightarrow \infty$ ,  $\xi \rightarrow \infty$  and  $\bar{v}_r \rightarrow \bar{v}$ .

In modeling the dynamics of the collision in the c.m., it seems most appropriate to consider the c.m. rms velocity of the particles; i.e.,

$$\begin{aligned}
(v^{*2})^{1/2} = v^* &= \left\{ \frac{\int_0^{\theta_0} \frac{2\eta}{\bar{v}} (\bar{v}^2 + \bar{v}_r^2 - 2\bar{v}_r \bar{v} \cos \theta) \sin \theta d\theta}{\int_0^{\theta_0} \frac{2\eta}{\bar{v}} \sin \theta d\theta} \right\}^{1/2} \\
&= \bar{v} \left\{ 1 + \frac{\bar{v}_r^2}{\bar{v}^2} - \frac{\bar{v}_r}{\bar{v}} (1 + \cos \theta_0) \right\}^{1/2} \\
&= \bar{v} \left\{ 1 + \left( \frac{1 + \cos \theta_0}{4} \right)^2 \right\}^{1/2}
\end{aligned}$$

The collision rate in an element of volume at  $r$  can best be determined by utilizing the rms velocity in the c.m. Each particle will make  $\sim \sigma N(r) v^*$  collisions per unit time, or the total number of scattering collisions is  $N^2(r) \sigma v^*$ .

Assuming the scattering is isotropic in the c.m. system and utilizing the same equations as developed in the previous section for the transformation from the c.m. to the spacecraft reference frame, we find the incremental flux striking the sphere at  $dA(\theta)$

$$dF_{ss} = dAS(\theta) \frac{N^2(r) \sigma v^*}{4\pi} \left\{ \sqrt{1 - \beta^2 \sin^2 \theta} + \frac{\beta^2 \cos^2 \theta}{\sqrt{1 - \beta^2 \sin^2 \theta}} - 2\beta \cos \theta \right\}^{1/2}$$

where in this instance

$$\beta = \frac{\bar{v}_r}{v^*}$$

and  $dAS(\theta)$  is the incremental solid angle subtended by  $dA$  as seen at  $r$ ; therefore,

$$dAS(\theta) = 2\pi \sin \theta d\theta$$

or



$$dF_{ss}(r) = 2\pi \int_0^{\theta_0} \frac{N^2(r) \sigma v^*}{4\pi} \left\{ \sqrt{1 - \beta^2 \sin^2 \theta} + \frac{\beta^2 \cos^2 \theta}{\sqrt{1 - \beta^2 \sin^2 \theta}} - 2\beta \cos \theta \right\} \sin \theta d\theta$$

$$= \frac{N^2(r) \sigma v^*}{2} \left\{ 1 - \beta \sin^2 \theta_0 - \cos \theta_0 \sqrt{1 - \beta^2 \sin^2 \theta_0} \right\}$$

Therefore, the total return flux from a solid shell  $dr$  at  $r$  from the sphere is

$$dF_{ss} = \frac{N^2(r) \sigma v^*}{2} H(\theta_0, \beta) 4\pi r^2 dr$$

where

$$H(\theta_0, \beta) = 1 - \beta \sin^2 \theta_0 - \cos \theta_0 \sqrt{1 - \beta^2 \sin^2 \theta_0}$$

or the total return flux to the sphere is

$$F_{ss} = \int_a^{\infty} dF_{ss}$$

Transforming to  $\theta_0$  coordinates,

$$r = \frac{a}{\sin \theta_0}$$

$$dr = \frac{-a \cos \theta_0 d\theta_0}{\sin^2 \theta_0}$$

or

$$F_{ss} = \int_0^{\pi/2} 2 \pi \sigma \left( \frac{2\eta}{\bar{v}} \right)^2 \bar{v} (1 - \cos \theta_o)^2 \left\{ 1 - \frac{(1 + \cos \theta_o)^2}{4} \right\}^{1/2} \left( \frac{a^3}{\sin^2 \theta_o} \right) \left\{ \frac{\cos \theta_o d \theta_o}{\sin^2 \theta_o} \right\} H(\theta_o, \beta)$$

where

$$\beta \equiv f(\theta_o)$$

The point at which  $\beta = 1$  is the coordinate beyond which no backscatter can occur, or

$$\beta = \frac{(1 + \cos \theta_o)}{2 \left( 1 - \frac{(1 + \cos \theta_o)^2}{4} \right)^{1/2}} \leq 1$$

$$\frac{1}{4} \frac{\sin^4 \theta_o + (1 + \cos \theta_o)^2 (1 - \cos \theta_o)^2}{(1 - \cos \theta_o)^2} \leq 1$$

$$\frac{\sin^4 \theta_o}{(1 - \cos \theta_o)^2} \leq 2$$

$$\cos \theta_o \leq \sqrt{2} - 1 \sim 0.414$$

$$90^\circ \leq \theta_o \leq \sim 65.5^\circ$$

Therefore, the backscatter flux per unit area striking the sphere is (note that  $R_o = a$  in our notation)

$$FT_{ss} = \frac{F_{ss}}{4\bar{\eta} a^2} \sim \frac{2\sigma\eta^2 R_0}{\bar{v}} \chi$$

$$\chi = \int_{\sim 65.5^\circ}^{90^\circ} (1 - \cos \theta)^2 \left(1 - \frac{(1 + \cos \theta)^2}{4}\right)^{1/2} \left(\frac{\cos \theta d\theta}{\sin^4 \theta}\right) (H(\theta, \beta)) \sim 10^{-2}$$

Utilizing the same values for the parameters as developed in the previous section, we find

$$FT_{ss} \sim 3 \times 10^5 / \text{cm}^2 \text{ s}$$

This flux is sufficiently less than those calculated in the previous section that it will be neglected in comparisons.

## V. FLUXES IN THE WAKE REGION DUE TO OTHER PHENOMENA

The direct emission/outgassing of molecules into the experimental area by the surrounding surfaces is one of the more important contributions to the flux density. As mentioned previously, an outgassing rate of  $10^{12}$  molecules/cm<sup>2</sup> s is assumed typical of spacecraft surfaces. However, a flux of  $10^{12}$ /cm<sup>2</sup> s is most typical of the outgassing rate of cured spacecraft paint or metals that have just been placed in a high vacuum system. An outgassing rate of from 0.2 to  $4 \times 10^7$  molecules/cm<sup>2</sup> s appears to be obtainable with some metals that have been vacuum outgassed for 20 h at 100°C [6,7] (a temperature that can be reached on the spacecraft surface during the sunlight portions of the orbit). In addition, the process of vacuum degassing may substantially lower the "intrinsic" outgassing rate of metals. For example, the outgassing rate of a sample of stainless steel was lowered from  $\sim 3 \times 10^8$  molecules/cm<sup>2</sup> s to  $3 \times 10^6$  molecules/cm<sup>2</sup> s by this technique [8]. Therefore, after an "in situ" bakeout, it may be possible to obtain fluxes due to metal outgassing of  $\sim 10^7$ /cm<sup>2</sup> s striking crucial components (e.g., substrates) of the experiment. This flux level may be additionally lowered by designing the apparatus so that items such as substrates are oriented toward the open aft end and only view a limited portion of the equipment/shield.

One of the areas about which very little is known is the influence of charging phenomena attracting the ambient ions onto a surface oriented toward the wake. A metal satellite body will typically charge up to approximately -1 V in an ionospheric orbit. This charging coupled with the generation of  $\vec{v} \times \vec{B}$  forces as the spacecraft traverses the Earth's geomagnetic field could result in potentials of approximately several volts on the satellite surface at specific portions of the orbit. Since the average energy of an ambient oxygen ion (in the spacecraft reference frame) is approximately 5 eV, this surface potential may be sufficient to deflect the ambient ions into the experimental area in the wake [9]. Additional work will have to be done to quantitatively assess the contributions to the flux in the wake from this phenomenon.

Another area of potential flux involved the emission of relatively large amounts of material during a melting distillation experiment. Depending upon the experiment envisioned, one could expect emission rates of from  $10^{16}$  to  $10^{20}$  particles/s. Utilizing the results developed in Section III, this may result in backscattering unacceptably large fluxes of ambient molecules into the experimental area. However, it should be noted that if the experiment utilizes a

source containing a low mass species such as boron, this backscattering flux is substantially reduced because an ambient oxygen cannot scatter directly into the wake surface with only one collision with a low mass particle.

Finally, the heat load occurring during the performance of an experiment will have to be distributed so as not to cause excessive outgassing of the experimental components. For the purpose of this report, we will assume that this can be accomplished in a straightforward manner by using good design and fabrication techniques. However, detailed measurements should be made to assess the effects of the heat load of various candidate experiments on the vacuum levels of the shield.

## VI. DISCUSSION

Based on the preliminary modeling described in the previous sections, the following tentative conclusions can be made regarding the contaminating fluxes impinging upon an experimental area placed in the wake zone of a satellite:

a. The hydrogen flux due to the direct ambient, which has sufficient velocity to overtake the space vehicle from the back, appears to be orders of magnitude greater than that backscattered. It would, therefore, appear that the atomic hydrogen in the wake can be calculated from local geophysical conditions and may be independent of spacecraft emission characteristics.

b. The backscattered ambient oxygen and helium fluxes, on the other hand, are substantially greater than the respective direct ambient fluxes. Therefore, it appears that the spacecraft emission characteristics and geometries can be a significant factor in determining the flux to an experiment located in the wake.

The fluxes to the experimental area of the direct ambient hydrogen and backscattered helium and oxygen were calculated to be  $\sim 10^7/\text{cm}^2 \text{ s}$  for the conditions mentioned previously. In addition, Section V discusses the possibility of conducting an experiment in the wake so that the critical components of the apparatus see a flux  $\sim 10^7/\text{cm}^2 \text{ s}$  due to material outgassing. Therefore, it appears that  $10^7/\text{cm}^2 \text{ s}$  may represent a lower limit to the flux level striking critical portions of the apparatus during a wake experiment.

It is interesting to compare the value of  $10^7/\text{cm}^2 \text{ s}$  to flux levels which may be desired by potential experiments that have been suggested as benefitting from the wake environment. A key operation of several of the experiments (e. g. , solar cell production and metal purification) is the physical vapor deposition of source material onto a substrate. Under certain optimal conditions it may be possible to obtain rapid deposition rates of  $\sim 10 \mu\text{m}/\text{min}$  buildup of full-density material on the substrate [10]. This rate is equivalent to a flux of  $\sim 10^{18}$  source atoms/ $\text{cm}^2 \text{ s}$  on the substrate. Therefore, a contaminating flux of  $10^7/\text{cm}^2 \text{ s}$  would mean an impurity level of 1 part in  $10^{11}$  due to interaction of the experiment with the environment.

The modeling done in Sections II and III is based on parameters associated with large unmanned spacecraft of the LDEF class. We would also like to calculate the fluxes which may be obtainable in the wake region behind large manned spacecraft (e. g. , the Shuttle). Based upon the contamination requirement specification of the Shuttle, one could anticipate column densities of

approximately  $3 \times 10^{13}/\text{cm}^2$  of  $\text{N}_2$ ,  $\text{O}_2$ , and  $\text{H}_2\text{O}$  above the Shuttle. This is equivalent to leakage/outgassing rates of approximately  $3 \times 10^{15}/\text{cm}^2 \text{ s}$  from the cabin/surface. Utilizing the equations/model developed in Section II, this will result in backscatter oxygen and helium fluxes of approximately  $3 \times 10^{10}/\text{cm}^2 \text{ s}$  to the experimental area. A backscattered flux of  $3 \times 10^{10}/\text{cm}^2 \text{ s}$  would result in an impurity level of 30 ppb for the example experiment discussed previously. This value of  $3 \times 10^{10}/\text{cm}^2 \text{ s}$  does not take into account factors such as the following which may reduce the value:

a. The inelastic scattering contribution to  $\sigma_{\text{Ao}}$  may be substantial given the molecular nature of the spacecraft emitted particles which are predominately  $\text{N}_2$ ,  $\text{O}_2$ , and  $\text{H}_2\text{O}$ .

b. The experiments could be performed on a surface held in an appropriate orientation at the end of the Shuttle remote manipulator unit (RMU). The 15 m length of the RMU would remove the disc from the immediate vicinity of the Shuttle, reducing the number of molecules that could backscatter onto the experiment.

c. Utilizing a portion of the Shuttle where the outgassing rate is not as severe.

Therefore, meaningful experiments utilizing the wake vacuum may be performed from the Shuttle under appropriate operating conditions which may include having the Shuttle in a gravity gradient stabilized mode to inhibit thruster firings during the experiment.

It should be noted that the order of magnitude ( $\sim 10^7$ ) of the fluxes calculated in this report for the wake region of unmanned spacecraft is roughly equivalent to those calculated to be present within a hemispherical shield. Obviously the geometrical shape of the wake shield does have the advantage of blocking some of both the direct and backscattered ambient particles from striking the working area in the center of the hemisphere. This can be deduced easily by observing the angular dependence of the fluxes presented in Tables 1 to 3. This may be an important consideration in utilizing the shield for certain classes of experiments. However, any type of quasi-spherical or conical shield does have two inherent limitations: (a) the experimental area will be subject to additional fluxes coming from the outgassing of the sides of the shield, and (b) the less than  $2\pi$  angle seen by an experiment in the shield implies a reduction in the inherent pumping speed of the space vacuum.

These limitations would be reduced when the experimental shield is opened, tending to the ultimate limit of a "flat" plate. However, the fluxes of direct and backscattered ambient particles are greater to a flat arrangement than to a hemisphere. The calculations developed in Sections II and III show that these fluxes can be of a sufficiently low level that meaningful experiments may be conducted on clean spacecraft.

Therefore, it appears that demonstration/precursor experiments can be initially conducted on presently planned space vehicles. In addition, it may be optimum to conduct the experiments on unmanned satellites. The LDEF series, for example, allows months of baking/outgassing in orbit before conducting the experiments which could be performed immediately before the LDEF is retrieved by the Shuttle. In addition, in its gravity gradient stabilized mode the LDEF orientation is such that the same surface always points into the wake. However, it should be noted that these precursor experiments might also be performed on manned space vehicles such as the Shuttle, although in this instance some restrictions would have to be placed on the operating conditions during the conduct of the experiment to obtain a sufficiently clean environment around the Shuttle.



## VII. CONCLUSIONS

The models derived in this report indicate that an experiment situated in the wake region of an unmanned spacecraft can see flux levels of  $\sim 10^7/\text{cm}^2 \text{ s}$  of H, He, and O due to the interaction between the spacecraft and the ambient atmosphere. For comparison, a flux of  $10^7/\text{cm}^2 \text{ s}$  (0 at 300°K) striking a surface corresponds to a pressure of  $\sim 2 \times 10^{-14}$  torr on the ground. The flux levels were obtained utilizing a model (3 m radius sphere) vehicle at an altitude of 550 km and having an emission rate of  $\sim 10^{12}/\text{cm}^2 \text{ s}$ .

After a mild bake similar to that which is naturally achieved in orbit, it may be possible to obtain fluxes  $\sim 10^7/\text{cm}^2 \text{ s}$  which are due to material outgassing and which strike critical experimental components. For components such as substrates, an orientation toward the open end of the shield may serve to reduce this flux. Therefore, it may be possible to obtain molecular fluxes  $\sim 10^7/\text{cm}^2 \text{ s}$  in an experimental area placed on the wake portion of a satellite. (One of the prerequisites would be having the wake experiment exposed and degassed in the space environment for a sufficiently long time that the fluxes from the experimental apparatus do not significantly degrade the wake vacuum.)

Similar calculations were made for a model having a large amount of surface emission (e. g. , the Shuttle). Under this condition, the vacuum environment is seriously degraded with a calculated flux of  $\sim 3 \times 10^{10}/\text{cm}^2 \text{ s}$  striking a surface normal to the wake axis.

The possibility of achieving such a high vacuum in the wake of presently available spacecraft would suggest an approach of doing simple investigative/precursor experiments on these vehicles. The results of these experiments would then be evaluated to assess the influence of various experimental parameters (such as the orbital altitude and the size/geometry of the shield) in designing a more permanent vacuum facility from which to conduct complex, ultrahigh vacuum experiments.

## REFERENCES

1. Proceedings AIAA/MSFC Symposium on Space Industrialization. Marshall Space Flight Center, Alabama, May 1976.
2. Wuenscher, H. F.: New Development in Space Manufacturing. Space Processing and Manufacturing Meeting, Marshall Space Flight Center, Alabama, October 1969.
3. Heuser, J. E. and Brock, F. J.: Theoretical Analysis of the Density within an Orbiting Wake Shield. *J. Vac. Sci. Tech.*, vol. 13, 1976, p. 702.
4. U. S. Standard Atmosphere Supplements, 1966. U. S. Government Printing Office, Washington, D. C.
5. Scialdone, S. S.: Molecular Fluxes from a Spacecraft Measured with Quartz Microbalances. *J. Vac. Sci. Tech.*, vol. 12, 1975, p. 569.
6. Moraw, G.: The Influence of Ionization Gauges on Gas Flow Measurements. *Vacuum*, vol. 23, 1974, p. 125.
7. Elsey, R. J.: Outgassing of Vacuum Materials - II. *Vacuum*, vol. 25, 1975, p. 347.
8. Horgan, A. M., and Dalins, I.: Hydrogen and Nitrogen Desorption Phenomena Associated with a Stainless Steel 304 Low Energy Electron Diffraction (LEED) and Molecular Beam Assembly. *J. Vac. Sci. Tech.*, vol. 9, 1972, p. 1218.
9. Oran, W. A.; Samir, U.; and Stone, N. H.: Parametric Study of the Near-Wake Structure of Spherical and Cylindrical Bodies in the Laboratory. *Planet. Space Sci.*, vol. 22, 1974, p. 379.
10. Bunshah, R.: Private communication.


## APPROVAL

# PRELIMINARY ASSESSMENT OF THE VACUUM ENVIRONMENT IN THE WAKE OF LARGE SPACE VEHICLES

By W. A. Oran and R. J. Naumann

The information in this report has been reviewed for security classification. Review of any information concerning Department of Defense or Atomic Energy Commission programs has been made by the MSFC Security Classification Officer. This report, in its entirety, has been determined to be unclassified.

This document has also been reviewed and approved for technical accuracy.

*for*   
\_\_\_\_\_  
CHARLES A. LUNDQUIST  
Director, Space Sciences Laboratory